The MHC class II transactivator affects local and systemic immune responses in an α-synuclein seeded rat model for Parkinson's disease

Filip Bäckström[1, 2, *], Itzia Jimenez-Ferrer[1], Kathleen Grabert[3], Lautaro Belifori[1], Kelvin C. Luk[4], Maria Swanberg[1]

[1]Translational Neurogenetics Unit, Department of Experimental Medical Science, Lund University, Lund, Sweden; [2]Inflammation and Stem Cell Therapy Group, Division of Clinical Neurophysiology, Department of Clinical Sciences, Lund University, Lund, Sweden; [3]Toxicology Unit, Institute of Environmental Medicine, Karolinska Institute, Stockholm, Sweden; [4]Center for the Neurodegenerative Disease Research, Department of Pathology and Laboratory Medicine, University of Pennsylvania Perelman School of Medicine, Pennsylvania, PA, USA

[*]Corresponding author

ABSTRACT

Parkinson's disease (PD) is characterized by intraneuronal inclusions of alpha-synuclein (α-Syn), neurodegeneration and a strong neuroinflammatory component. Studies have shown that genetic variants affecting quantity and quality of major histocompatibility complex II (MHCII) have implications in PD susceptibility and that PD patients have α-Syn specific T lymphocytes in circulation. The class II transactivator (CIITA) is the major regulator of MHCII expression and reduced CIITA expression has been shown to significantly increase α-Syn induced neurodegeneration and pathology in an α-Syn overexpression rat model combined with α-Syn pre-formed fibrils (PFF). In this study, we characterized immune profiles associated with the enhanced PD-like pathology observed in congenic rats with *Ciita* allelic variants causing lower CIITA levels compared to the background strain. Flow cytometry showed that rats with lower CIITA levels had an increased proportion of MHCII+ microglia and circulating myeloid cells, yet lower levels of MHCII on individual cells. Additionally, lower CIITA levels were associated to higher TNF levels in serum, trends of higher CD86 levels in circulating myeloid cells and a lower CD4/CD8 T lymphocyte ratio in blood. Taken together, these results indicate that CIITA regulates susceptibility to PD-like pathology through baseline immune populations and serum TNF levels.

33 INTRODUCTION

34 Parkinson's disease (PD) is a progressive and incurable neurodegenerative disorder estimated
35 to affect 2-3% of the population above the age of 65[1]. PD is very heterogenous and
36 approximately 95% of all cases have a multifactorial etiology where genetics, lifestyle and
37 environment are contributing factors[2]. A characteristic feature of PD is the degeneration of
38 dopaminergic neurons in the substantia nigra pars compacta (SN), intraneuronal inclusions of
39 alpha-synuclein (α-Syn) and neuroinflammation[3]. The neuroinflammatory process in PD
40 includes microglial activation, local upregulation of major histocompatibility complex II
41 (MHCII), altered levels of pro-inflammatory cytokines in cerebrospinal fluid (CSF), as well as
42 systemic changes in blood cytokine levels and lymphocyte populations[3]. Genetic association
43 studies have identified single nucleotide polymorphisms in the human leukocyte antigen
44 (*HLA*) locus that regulate the expression of MHCII to be associated with an increased risk of
45 developing PD[4,5]. Recently, coding polymorphisms causing amino-acid changes in *HLA-D*
46 haplotypes (*HLA-DRB1*4*) were also shown to be associated to PD with a protective effect[6].
47 Collectively, this indicates that both the quantity and quality of MHCII affect the risk of
48 developing PD. Since MHCII molecules present antigens to T lymphocytes and induce antigen-
49 specific responses they serve as a link between the innate and adaptive immune systems[7].
50

51 A role of the adaptive immune system in PD etiology is supported by the presence of
52 lymphocytes in post-mortem brain tissue from PD patients[8] and findings of α-Syn reactive
53 CD4+ lymphocytes[9,10] early in the disease process[11]. However, it is not clear if and how
54 antigen presentation contributes to or protect from PD pathology. The level of MHCII on
55 antigen-presenting cells is controlled by the class II transactivator (CIITA, also known as
56 MHC2TA) and silencing of *Ciita in vivo* using shRNA has been shown to prevent
57 neurodegeneration in a nigral α-Syn overexpression model of PD in mice[12]. In contrast, we
58 have previously found that rats with naturally occurring variants in the promotor of *Ciita* and
59 lower MHCII levels have more widespread α-Syn pathology and more activated microglia
60 after nigral overexpression of α-Syn alone[13] and combined with striatal seeding with α-Syn
61 pre-formed fibrils (PFF)[14]. Of note, genetic variants mediating lower CIITA expression are also
62 found in humans and are associated with increased susceptibility to multiple sclerosis,

63 rheumatoid arthritis and myocardial infarction, further adding to the interest of studying
64 CIITA in relation to PD[15].
65
66 The aim of this study was to investigate the effect of CIITA and MHCII expression on peripheral
67 and local immune responses during α-Syn seeded PD-like pathology. To do so, we used a
68 recombinant adeno-associated viral vector (rAAV) nigral α-Syn overexpression rat model
69 combined with striatal seeding of human PFF in two congenic rat strains with different
70 transcriptional activity of the *Ciita* gene. Using a flow cytometric approach, we investigated
71 both resident and peripheral immune populations and confirmed previous results that rats
72 with lower levels of CIITA have less MHCII expression in microglial cells compared to wild-type
73 (wt) rats. Importantly, rats with lower CIITA expression also had lower MHCII levels and trends
74 of higher levels of the co-stimulatory marker CD86 in circulating myeloid cells as well as higher
75 levels of tumor necrosis factor (TNF) in serum. Collectively these results suggest that the levels
76 of CIITA alter immune populations, immune responses and cytokine levels that in turn could
77 affect the susceptibility to PD.

78 ## RESULTS

79 ### The rAAV-α-Syn+PFF PD model results in robust α-Syn expression, α-Syn inclusions and
80 dopaminergic neurodegeneration

81 To investigate the effects of differential expression of CIITA on PD like-pathology we used wt
82 DA rats and a congenic DA.VRA4 rat strain with lower expression levels of CIITA and MHCII[13].
83 Rats were injected with a rAAV6-α-Syn vector[16] into the SN followed by an injection of
84 sonicated human α-Syn PFF two weeks later in the striatum (rAAV-α-Syn+PFF, α-Syn group)
85 (Fig. 1a, b). Control animals were injected with an empty rAAV6 vector into the SN and vehicle
86 (Dulbecco's phosphate buffered saline (DPBS)) into the striatum (rAAV-(-)+DPBS, control
87 group). Rats were sacrificed at baseline (naïve), 4- or 8-weeks post nigral injection for
88 collection of brain, blood and CSF samples (Fig. 1a).
89
90 Neurodegeneration and α-Syn pathology in the rAAV-α-Syn+PFF model used have been
91 thoroughly characterized in a previous study[14]. Qualitative histological assessment confirmed
92 robust positive signal of human α-Syn in the SN and striatum of both DA and DA.VRA4 rats in
93 4- and 8-week α-Syn groups (Fig. 1c and Supplementary Fig. 1a). Controls did not show any

94 human α-Syn signal (Supplementary Fig. 1b, c). As expected, the rAAV-α-Syn+PFF model
95 resulted in loss of tyrosine hydroxylase (TH) positive signal in both DA and DA.VRA4 rats at 4-
96 and 8-weeks (Fig. 1d and Supplementary Fig. 1d) whereas the TH-positive signal remained
97 intact in the control groups (Supplementary Fig. 1e, f). The unilateral rAAV-α-Syn+PFF model
98 also resulted in pathological forms of α-Syn aggregates, represented by phosphorylated α-
99 Syn at Serine residue 129 (pS129) in the cell soma and in neurites (Fig. 1e) as well as by
100 proteinase K-resistant α-Syn aggregates mainly observed as puncta along neurites (Fig. 1f) in
101 ipsilateral, but not contralateral hemispheres (Supplementary Fig. 1g-h). Additionally, rAAV-
102 α-Syn+PFF lead to upregulation of MHCII molecules in the ipsilateral but not contralateral
103 midbrain of both the DA and DA.VRA4 rats (Fig. 1g and Supplementary Fig. 1i).
104

105 The rAAV-α-Syn+PFF PD model induces microglial MHCII+ expression and CSF cytokine levels
106 in DA and DA.VRA4 rats

107 We have previously revealed that DA.VRA4 rats with lower levels of CIITA have more activated
108 microglia compared to DA in α-Syn based PD-models[13,14]. However, this data was based on
109 immunohistochemistry (IHC) that has limited capacity to identify cell populations. By applying
110 flow cytometric analysis of brain cells, we found a similar percentage of microglia
111 ($CD45^{dim}CD11b+$) in control and α-Syn groups (~93-97%) (Fig. 2a and Supplementary Fig. 2a,
112 b). There was, however, an increased percentage of MHCII+ microglial cells in the ipsilateral
113 compared to contralateral hemisphere in both control and α-Syn groups at 4 weeks (DA
114 control 6.8 ± 2.0% vs 4.2 ± 0.99%, p=0.0080, 95% CI [1.0, 4.1]; DA α-Syn 14 ± 4.0% vs 4.8 ±
115 0.81%, p=0.0010, 95% CI [5.5, 13]; DA.VRA4 control 7.0 ± 1.3% vs 4.8 ± 0.72%, p=0.0070, 95%
116 CI [0.90, 3.5]; DA.VRA4 α-Syn 12 ± 3.2% vs 5.0 ± 1.7%, p=0.0010, 95% CI [4.0, 9.2]) and 8 weeks
117 (DA control 7.0 ± 1.3% vs 5.3 ± 1.5%, p=0.026, 95% CI [0.31, 3.1]; DA α-Syn 8.5 ± 1.8% vs 4.4
118 ± 0.87%, p=0.0020, 95% CI [2.6, 5.8]; DA.VRA4 control 6.7 ± 0.73% vs 5.3 ± 0.90%, p<0.0010,
119 95% CI [0.88, 1.9]; DA.VRA4 α-Syn 8.4 ± 1.3% vs 4.7 ± 0.98%, p<0.0010, 95% CI [2.9, 4.3])
120 (Supplementary Fig. 2c). By comparing normalized values (ipsilateral/contralateral), the
121 increase in MHCII+ microglial cells was larger in the α-Syn groups compared to controls in
122 both strains at 4 weeks (DA 2.9 ± 0.61 vs 1.6 ± 0.35, p=0.0012, 95% CI [0.65, 1.9]; DA.VRA4
123 2.4 ± 0.71 vs 1.5 ± 0.28, p=0.012, 95% CI [0.26, 1.6]) and at 8 weeks (DA 2.0 ± 0.30 vs 1.4 ±
124 0.28, p=0.0069, 95% CI [0.21, 1.0]; DA.VRA4 1.8 ± 0.17 vs 1.3 ± 0.12, p=00030, 95% CI [0.31,

125 0.71]) (Fig. 2b). The levels of MHCII (determined by median fluorescence intensity, MFI) on
126 microglia were also elevated in the ipsilateral compared to contralateral hemisphere in
127 response to α-Syn at 4 weeks in both strains (DA 2,600 ± 456 MFI vs 1,895 ± 131 MFI,
128 p=0.0040, 95% CI [344, 1,065]; DA.VRA4 2,075 ± 267 MFI vs 1,684 ± 163 MFI, p=0.038, 95% CI
129 [33, 749]) whereas it returned to control levels at 8 weeks in both strains (Supplementary Fig.
130 2d). After normalizing MHCII+ MFI values (ipsilateral/contralateral) the relative levels was
131 higher in the α-Syn group compared to control at 4 weeks (DA 1.4 ± 0.17 vs 0.98 ± 0.19,
132 p=0.0039, 95% CI [0.15, 0.61]; DA.VRA4 1.2 ± 0.22 vs 0.99 ± 0.097, p=0.028, 95% CI [0.034,
133 0.47]) but not at 8 weeks (Fig. 2c). We did not observe any changes in infiltrating
134 macrophages/monocytes ($CD45^{high}CD11b+$) populations in brain (Fig. 2a) in terms of overall
135 percentage or percentage of MHCII+ macrophages (Supplementary Fig. 2e-f). The MHCII+ MFI
136 level of infiltrating macrophages/monocytes was higher in the ipsilateral compared to
137 contralateral hemisphere at 4 weeks in the α-Syn group of DA.VRA4 rats (15,210 ± 1,896 MFI
138 vs 13,870 ± 1,729 MFI, p=0.019, 95% CI [330, 2,338]) (Supplementary Fig. 2g, right).
139
140 CD86 (also known as B7-2) is a co-stimulatory signal expressed by antigen-presenting cells
141 necessary for activation of T lymphocytes[7]. The rAAV-α-Syn+PFF model or control did not
142 change CD86 MFI levels in macrophages in the ipsilateral hemisphere (Supplementary Fig.
143 2h). Microglial CD86 MFI values were lower in the ipsilateral compared to contralateral
144 hemisphere at 4 weeks in the α-Syn group in both strains (DA 714 ± 30 MFI vs 784 ± 53 MFI,
145 p=0.0070, 95% CI [-111, -29]; DA.VRA4 713 ± 114 MFI vs 774 ± 93 MFI, p=0.0050, 95% CI [-93,
146 -29]), at 8 weeks in the control groups (DA 1,115 ± 169 MFI vs 1,182 ± 159 MFI, p=0.021, 95%
147 CI [-117, -15]; DA.VRA4 1,053 ± 128 MFI vs 1,085 ± 143 MFI, p=0.029, 95% CI [-57, -4.9] and
148 at 8 weeks in the DA α-Syn group (924 ± 64 MFI vs 1,018 ± 43 MFI, p=0.0050, 95% CI [-140, -
149 48]) (Supplementary Fig. 2i). After normalization to the contralateral hemisphere, the relative
150 CD86 MFI levels were reduced in the DA α-Syn group compared to control at 4 weeks only
151 (0.91 ± 0.0046 vs 0.99 ± 0.073, p=0.042, 95% CI [-0.16, -0.0038) (Fig. 2d). Additionally, there
152 was a slight increase in infiltrating T lymphocytes (CD45+CD3+) in the ipsilateral compared to
153 contralateral hemisphere at 4 weeks in the DA α-Syn group (0.96 ± 0.36% vs 0.65 ± 0.25%,
154 p=0.032, 95% CI [0.039, 0.57]), DA.VRA4 control (1.0 ± 0.19% vs 0.77 ± 0.32%, p=0.034, 95%
155 CI [0.030, 0.53]) and DA.VRA4 α-Syn (1.2 ± 0.40% vs 0.73 ± 0.24%, p=0.0040, 95% CI [0.26,

156 0.77]) (Fig. 2e). These results indicate that there is early infiltration of T lymphocytes but no
157 upregulation of the co-stimulatory marker CD86 necessary for T lymphocyte activation in the
158 rAAV-α-Syn+PFF rat model for PD.
159
160 Altered levels of cytokines in the CSF are reported in PD patients[3]. To investigate the effect of
161 rAAV-α-Syn+PFF on CSF cytokine levels, we performed multiplexed ELISA. Compared to
162 control, CSF cytokine levels were unaffected in α-Syn groups at 4 weeks (Fig. 2f), but
163 increased at 8 weeks; TNF in DA rats (0.41 ± 0.18 pg/ml vs 0.20 ± 0.19 pg/ml, p=0.049, 95% CI
164 [0.00060, 0.42]) and IL-6 in both DA (44 ± 21 pg/ml vs 12 ± 12 pg/ml, p=0.0029, 95% CI [13,
165 52]) and DA.VRA4 (31 ± 11 pg/ml vs 6.6 ± 7.6 pg/ml, p=0.00020, 95% CI [14, 35]) (Fig. 2g).
166
167 The rAAV-α-Syn+PFF PD model induces changes in blood myeloid- and T lymphocyte
168 populations
169 To investigate changes in peripheral immune cell populations, we performed flow cytometry
170 of blood collected 4- and 8-weeks post nigral injection (Supplementary Fig. 3a). At 4 weeks,
171 we observed lower levels of circulating myeloid cells (CD45+CD11b+) in DA rats injected with
172 rAAV-α-Syn+PFF compared to controls (20 ± 4.4% vs 27 ± 3.4%, p=0.012, 95% CI [-12, -2.0])
173 (Fig. 3a, b), but a higher percentage were MHCII+ (9.0 ± 1.4% vs 7.0 ± 1.4%, p=0.036, 95% CI
174 [0.16, 3.7]) (Fig. 3c). The overall percentage of T lymphocytes, CD4+ T lymphocytes or
175 CD4/CD8 ratio did not change in response to α-Syn in DA or DA.VRA4 rats (Supplementary
176 Fig. 3b, c and Fig. 3e). There was, however, a higher percentage of CD8+ T lymphocytes in DA
177 -α-Syn rats compared to controls at 8 weeks (37 ± 7.3% vs 28 ± 4.9%, p=0.047, 95% CI [0.16,
178 18]) (Fig. 3f).
179
180 To investigate blood cytokine levels, we performed multiplexed ELISA on serum. The rAAV-α-
181 Syn+PFF model lead to higher levels of IL-1β (23 ± 6.7 pg/ml vs 14 ± 5.8 pg/ml, p=0.022, 95%
182 CI [1.5, 16]) and IL-5 (37 ± 5.8 pg/ml vs 29 ± 4.2 pg/ml, p=0.0077, 95% CI [2.7, 14]) in DA.VRA4
183 rats compared to controls at 4 weeks, but no changes at 8 weeks or in DA rats (Fig. 3g, h).
184

185 Differential expression of CIITA regulates MHCII levels on brain macrophages and microglia
186 during rAAV-α-Syn+PFF induced pathology
187 Since DA.VRA4 rats with lower CIITA levels are more susceptible to α-Syn pathology and
188 dopaminergic neurodegeneration than DA rats[14], we compared immune cell populations by
189 flow cytometry of brain tissue between the strains. DA and DA.VRA4 rats injected with rAAV-
190 α-Syn+PFF did not differ in terms of microglial population size, proportion of MHCII+ microglia
191 (Fig. 4a, b) or infiltration of T lymphocytes (Supplementary Fig. 4a). However, naïve DA.VRA4
192 rats had, compared to DA, a lower percentage of microglia (93 ± 1.9% vs 96 ± 1.1%, p=0.017,
193 95% CI [-5.1, -0.65]) but increased percentage of MHCII+ microglia (5.7 ± 0.60% vs 4.9 ± 0.35%,
194 p=0.019, 95% CI [0.18, 1.6]) (Fig. 4a, b). In line with previous IHC-based data, the intensity of
195 the MHCII+ signal (ipsilateral MFI normalized to contralateral MFI for DA) on microglia was
196 lower in DA.VRA4 rats compared to DA (Fig 4c). This CIITA-dependent difference was
197 observed between DA.VRA4 and DA naïve (0.88 ± 0.032 vs 0.97 ± 0.077, p=0.029, 95% CI [-
198 0.17, -0.011]), 8-week control (0.95 ± 0.038 vs 1.0 ± 0.030, p=0.0014, 95% CI [-0.13, -0.042]),
199 α-Syn 4 weeks (1.1 ± 0.097 vs 1.4 ± 0.19, p=0.011, 95% CI [-0.47, -0.079]) and α-Syn 8 weeks
200 (0.91 ± 0.072 vs 1.0 ± 0.063, p=0.016, 95% CI [-0.23, -0.031]) (Fig. 4c). There were no
201 differences between DA and DA.VRA4 rats in percentages of brain macrophages or MHCII+
202 brain macrophages (Fig. 4d, e). However, brain macrophages from DA.VRA4 rats with reduced
203 CIITA levels had lower levels of MHCII compared to DA naïve (0.76 ± 0.15 vs 1.0 ± 0.094,
204 p=0.010, 95% CI [-0.42, -0.073]), α-Syn 4 weeks (0.76 ± 0.061 vs 1.0 ± 0.046, p<0.00010, 95%
205 CI [-0.34, -0.21]) and α-Syn 8 weeks (0.92 ± 0.047 vs 1.1 ± 0.081, p=0.0080, 95% CI [-0.24, -
206 0.050]) (Fig. 4f).
207
208 Microglial CD86 levels (ipsilateral MFI values normalized to contralateral MFI values for DA)
209 did not differ between strains (Fig. 4g). Similarly, brain macrophage CD86 MFI levels did not
210 differ between DA and DA.VRA4 rats except for the 4 week control groups, where DA.VRA4
211 had lower CD86 MFI compared to DA (1.0 ± 0.13 vs 1.2 ± 0.076, p=0.032, 95% CI [-0.28, -
212 0.016]) (Fig. 4h).
213

214 No differences in CSF cytokine levels were observed between the two strains apart from
215 higher IL-10 levels in DA.VRA4 compared to DA rats in the α-Syn 8 week group (3.2 ± 1.1 pg/ml
216 vs 1.7 ± 0.74 pg/ml, p=0.0084, 95% CI [0.42, 2.4]) (Supplementary Fig. 4b-d).
217
218 Lower CIITA expression is associated with increased percentage of blood MHCII+ myeloid cells,
219 decreased CD4/CD8 ratio and elevated TNF levels in serum
220 We used flow cytometric analyses of myeloid cells and CD4+/CD8+ T lymphocytes to
221 determine if differential expression of CIITA affects circulating immune cells in naïve, control
222 and α-Syn groups of DA and DA.VRA4 rats. There was no difference between rat strains in
223 overall percentage of circulating myeloid cells (Fig. 5a). Similar to the results from brain, naïve
224 DA.VRA4 rats with lower CIITA levels had a higher percentage of MHCII+ myeloid cells in blood
225 compared to DA (12 ± 2.6% vs 7.0 ± 2.9%, p=0.0071, 95% CI [1.8, 8.9]) (Fig. 5b). Also similar
226 to the results from brain, myeloid cells in blood from DA.VRA4 showed a trend of lower MHCII
227 levels, determined by normalized MFI values for DA, and this was independent of intervention
228 (Fig. 5c). Opposite to infiltrating myeloid cells in brain, blood myeloid cell CD86 levels (MFI
229 values normalized for DA) were higher in DA.VRA4 compared to DA rats, although only
230 significantly higher in the control group at 4 weeks (1.6 ± 0.48 vs 1.0 ± 0.084, p=0.014, 95% CI
231 [0.15, 1.0]) (Fig. 5d).
232
233 Even though we did not observe a difference in overall percentage of T lymphocytes in blood
234 in response to α-Syn, the percentage was lower in DA.VRA4 rats compared to DA at 4 weeks
235 in the α-Syn group (49 ± 6.8% vs 59 ± 5.6%, p=0.021, 95% CI [-18, -1.9]) (Fig. 5e). Investigating
236 T lymphocyte subpopulations, the percentage of CD4+ cells was lower in DA.VRA4 rats
237 compared to DA in both naïve (70 ± 2.5% vs 74 ± 1.4%, p=0.0037, 95% CI [-7.0, -1.8]) and the
238 8 week control group (59 ± 4.9% vs 66 ± 3.2%, p=0.024, 95% CI [-13, -1.2]) whereas CD8+ T
239 lymphocytes were increased in naïve DA.VRA4 rats compared to DA (27 ± 1.5% vs 23 ± 1.4%,
240 p=0.0023, 95% CI [1.5, 5.2]) (Fig. 5f-g). Consequently, a reduced CD4/CD8 ratio was observed
241 in DA.VRA4 compared to DA rats in both naïve (2.6 ± 0.21 vs 3.2 ± 0.26, p=0.0019, 95% CI [-
242 0.87, -0.27]) and the 8 week control group (1.8 ± 0.37 vs 2.4 ± 0.50, p=0.036, 95% CI [-1.2, -
243 0.055]) (Fig. 5h). The differences in T lymphocyte subpopulations in rats with differing CIITA
244 levels were, thus, not depending on α-Syn.

Naïve DA.VRA4 rats with lower levels of CIITA had higher levels of TNF in serum compared to DA (4.2 ± 0.57 pg/ml vs 3.3 ± 0.56 pg/ml, p=0.022, 95% CI [0.15, 1.6]), and this difference remained in control- (4-week 2.7 ± 0.37 pg/ml vs 2.0 ± 0.16 pg/ml, p=0.0012, 95% CI [0.31, 0.98], 8-week 4.3 ± 0.58 pg/ml vs 3.1 ± 0.36 pg/ml, p=0.00060, 95% CI [0.64, 1.8]) and α-Syn groups (4-week 2.4 ± 0.56 pg/ml vs 1.9 ± 0.22 pg/ml, p=0.039, 95% CI [0.030, 1.0], 8-week 4.3 ± 0.40 pg/ml vs 3.1 ± 0.43 pg/ml, p=0.00020, 95% CI [0.71, 1.7]) (Fig. 5i-k). Additionally, DA.VRA4 rats had higher levels of IL-1β compared to DA for naïve (29 ± 14 pg/ml vs 11 ± 8.3 pg/ml, p=0.025, 95% CI: [2.8, 33]) (Fig. 5i) and higher IL-5 levels for α-Syn 4 weeks (37 ± 5.8 pg/ml vs 25 ± 11 pg/ml, p=0.019, 95% CI [2.5, 23]) (Fig. 5j, right).

DISCUSSION

Studies investigating human cohorts and experimental models support a role for antigen presentation and adaptive immune responses in PD etiology. However, there are contradictory findings on how local and peripheral immune responses contribute to or protect against different aspects of PD. Contributing factors to these discrepancies likely include difficulties in determining causality versus consequence in an ongoing pathological process, as well as the multiple different murine models used to study PD-related changes in the immune system. In a recent study, we showed that lower CIITA levels are associated with increased susceptibility to α-Syn pathology and dopaminergic neurodegeneration in the rAAV-α-Syn+PFF PD model[14]. This strongly supports CIITA, MHCII and the process of antigen presentation to have causal impact on PD risk and outcome. The relative contribution of resident/local (brain) and peripheral (systemic) immune cells and cytokines in this process is, however, not known. Therefore, in the current study we have characterized the effects of CIITA expression levels on local and peripheral immune populations in the rAAV-α-Syn+PFF model.

To assess the role of antigen presentation in PD-like pathology, we have used rats with naturally occurring variants in the *Ciita* gene, leading to differential expression of MHCII. Genetic variants regulating *Ciita* expression are found in multiple rat strains and in humans, where the orthologue regulates MHCII expression and are associated with susceptibility to rheumatoid arthritis, multiple sclerosis and myocardial infarction[15]. We argue that these

276 congenic rats provide a physiologically highly relevant model to study the effects of antigen
277 presentation on immune populations and PD-like pathology. This is in sharp contrast to the
278 use of knockout (KO) models with dysfunctional immune systems to study the role of
279 immune-related proteins or molecules[8,12,17-21].
280
281 Even though there is substantial evidence of the involvement of *HLA*/MHCII in PD indicated
282 by genetic association studies and elevated MHCII levels at the site of neurodegeneration[3-
283 6,22,23], the knowledge on the role of MHCII in disease etiology is lacking. Moreover, the results
284 from animal models are somewhat contradictory, probably due to the different
285 methodologies used to study the impact of MHCII and CIITA on PD-like pathology. The various
286 approaches include different species (rats[13,14,24] or mice[12,21,25]), different models of
287 PD/synucleinopathies (transgenic[21], rAAV-α-Syn[12,13,24,25], or rAAV-α-Syn+PFF[14]) and the
288 approach on how to manipulate CIITA/MHCII levels or the adaptive immune system (KO
289 models[12,21,25], nude rats[24], silencing through shRNA[12], or the use of congenic strains[13,14]). The
290 model employed in the current study has high construct validity (common *CIITA* genetic
291 variants regulate MHCII levels both in rats and humans) and high face validity (the rAAV-α-
292 Syn+PFF rat model displays seeded α-Syn pathology, dopaminergic neurodegeneration,
293 motor impairment and neuroinflammation). Together, these characteristics allow for a good
294 predictive validity of the model.
295
296 Our results are partly contradictory to other *in vivo* studies of CIITA impact on PD-like
297 pathology, but differences in the respective *in vivo* models are important to consider. In mice,
298 silencing of *Ciita* through shRNA reduced T lymphocyte and monocyte infiltration and
299 protected against SN dopaminergic loss upon nigral rAAV-α-Syn overexpression[12]. However,
300 the silencing of *Ciita* was also associated with a significant reduction of MHCII+ microglia cells
301 ($CD45^{dim}CD11b+$)[12]. Other studies found that complete KO of MHCII or CIITA fully protected
302 against dopaminergic cell loss[12,25] and microglial activation[25] in response to α-Syn
303 overexpression. In one study KO of MHCII resulted in accelerated pathology in the brain and
304 an overall reduction of T lymphocytes in the CNS of transgenic mice expressing human α-Syn
305 with the A53T mutation (M83+/0) combined with injection of PFF into the hindlimb[21]. The KO
306 of MHCII or CIITA creates a dysfunctional immune system and lost interplay between CD4+ T

307 lymphocytes and antigen presenting cells that limits the physiological relevance of these
308 models. In rats, T lymphocyte deficient (homozygous nude) rats did not upregulate MHCII
309 levels in response to nigral rAAV-α-Syn injection and were partially protected against
310 dopaminergic cell loss compared to heterozygous nude rats[24]. Interestingly, there was no
311 difference in α-Syn pathological load in SN between homozygous and heterozygous nude rats,
312 which may be influenced by the fact that heterozygous nude rats have significantly fewer T
313 lymphocytes compared to wt rats.
314
315 Using flow cytometry, this study confirms previous semi-quantitative findings from brain
316 immunostaining and RT-qPCR regarding microglial MHCII expression in response to α-Syn;
317 lower CIITA levels are associated to a larger proportion of microglia expressing MHCII but with
318 lower levels of MHCII per cell[13,14]. Additionally, by analyzing blood, we show that lower CIITA
319 levels in naïve DA.VRA4 rats affect MHCII expression in circulating cells of the myeloid lineage
320 in a similar way as in microglia; a higher percentage is MHCII+ but the MHCII level per cell is
321 lower. Thus, differential expression/levels of *Ciita* affects the baseline levels of MHCII+
322 microglia and MHCII+ circulating myeloid cells, and not only after initiation of PD like
323 pathology[12-14]. We hypothesize that increased numbers of MHCII+ microglia could accelerate
324 dopaminergic neurodegeneration through pathological spread of α-Syn, as we have
325 previously reported an increased aggregation and propagation of α-Syn in DA.VRA4 rats,
326 along with pathological α-Syn (pS129) co-localized within MHCII+ microglial cells in the rAAV-
327 α-Syn+PFF model[14] (Fig. 6).
328
329 Compared to studies using α-Syn nigral overexpression or striatal PFF injection in mice[12,26,27],
330 we found very limited numbers of brain infiltrating macrophages/monocytes and
331 lymphocytes in the rAAV-α-Syn+PFF rat model. Among live cells analyzed from brain tissue,
332 93-97% were $CD45^{dim}$CD11b+ microglia and only 0.5-1.5% $CD45^{high}$CD11b+
333 macrophages/monocytes. However, as much as 70-85% of the macrophages/monocytes but
334 only 5-15% of the microglia were MHCII+, indicating that infiltrating macrophages/monocytes
335 might still play an active role in CNS antigen presentation. The low number of infiltrating
336 macrophages/monocytes and lack of differences between α-Syn and control groups in this
337 model is contradictory to a previous study reporting that PD-like pathology was mainly driven

338 by infiltrating monocytes in a nigral α-Syn overexpression model in mice[20]. In addition, CIITA
339 levels did not affect the number of infiltrating macrophages/monocytes or lymphocytes in
340 our model, while KO and silencing of *Ciita* have been reported to greatly reduce both
341 monocyte and lymphocyte infiltration in mice overexpressing α-Syn in SN[12].
342
343 As for T lymphocytes (CD45+CD3+) infiltrating the brain, we recorded few events from brain
344 tissue, and while infiltration of T lymphocytes increased after rAAV-α-Syn+PFF injection at 4
345 weeks, this response was not dependent on CIITA levels. This finding suggests that T
346 lymphocyte infiltration mainly occurs at early stages, prior to any major neurodegeneration,
347 which has been reported in other murine PFF models[27,28]. In blood, DA.VRA4 rats had fewer
348 T lymphocytes in circulation compared to DA at 4 weeks in response to α-Syn. We also
349 observed a reduced CD4/CD8 ratio in blood from naïve DA.VRA4 rats with lower CIITA levels,
350 driven by a decrease in CD4+ and increase in CD8+ T lymphocytes, although this difference
351 was not seen between rats receiving rAAV-α-Syn+PFF injections.
352
353 Studies in α-Syn-based PD models indicate both detrimental and protective roles of
354 lymphocytes. Neurodegeneration-promoting effects are supported by findings that mice
355 lacking lymphocytes (*Rag1* KO) were protected against dopaminergic cell loss in SN, that
356 lymphocyte reconstitution resulted in dopaminergic cell loss comparable to wt mice[29] and
357 that CD4 KO protected against neurodegeneration in the SN and inhibited myeloid
358 activation[19]. In contrast, protective effects of lymphocytes have been reported in a striatal α-
359 Syn PFF model, where adoptive transfer of CD4+ lymphocytes to immunocompromised mice
360 reduced α-Syn pathology[18]. Studies on lymphocyte populations in PD patients are also
361 inconclusive. A recent study reported no difference in T lymphocytes overall or in
362 subpopulations (CD4+ or CD8+), but a reduction in effector and regulatory T lymphocytes in
363 PD[30]. Others report a decrease in T lymphocytes overall, and in both CD4+ and CD8+
364 subpopulations[31]. Additionally, there are reports on a lower CD4/CD8 ratio in PD patients due
365 to decreased numbers of CD4+ lymphocytes[32] and on an overall decrease in circulating CD4+
366 lymphocyte subpopulations due to decreased levels of T-helper (Th) 2, Th17 and regulatory
367 lymphocytes[33]. Other research suggests an overall decrease in circulating lymphocytes with
368 increased Th1 and Th17 but decreased Th2 and regulatory T lymphocytes[34] or no changes in

369 Th1 and Th2 subsets but an increase in the Th17 lymphocyte population[35]. In addition to
370 differences in population sizes and ratios, functional studies indicate altered functions of
371 lymphocyte populations in PD. One study found deficits in migratory capacity of CD4+ T
372 lymphocytes from PD patients[36]. Another study reported impaired suppressor functions of T
373 regulatory cells in PD, which could be resorted by *ex vivo* expansion[30]. A third study reported
374 that higher level of activation of T lymphocytes in response to phytohemagglutinin
375 stimulation was associated with PD disease severity[31]. To decipher the contribution of T
376 lymphocytes on PD susceptibility and progression more studies on the role of T lymphocytes
377 and MHC-dependent immune responses in PD are required.
378
379 In addition to altered immune cell profiles, we found alterations in CSF and serum levels of
380 several cytokines with possible links to PD. The rAAV-α-syn+PFF model resulted in increased
381 CSF IL-6 levels in both DA and DA.VRA4 rats. These results are in line with clinical findings in
382 which elevated CSF IL-6 levels were observed in PD patients[37]. We also found higher levels of
383 the anti-inflammatory cytokine IL-10 in CSF from DA.VRA4 rats compared to DA (8-week α-
384 syn), which has previously been shown to be neuroprotective and reduce microglial activation
385 in toxin models of PD[38]. Higher serum levels of IL-5, reported to be elevated in CD4+ Th2
386 lymphocytes from PD patients stimulated with α-Syn peptides *ex vivo*[10], were also found in
387 the DA.VRA4 α-Syn group compared to control. Increased IL-1β and TNF levels in blood have
388 been seen in PD patients from multiple studies[39], and we found higher levels of TNF in serum
389 in DA.VRA4 compared to DA and higher levels of IL-1β in DA.VRA4 α-Syn compared to control.
390 IL-1β levels have also been shown to influence the NLRP3 inflammasome and contribute to
391 neurodegeneration in a 6-OHDA mouse model of PD[40] and correlate to disease progression
392 in PD patients[41]. Together with our previous findings, it is possible that elevated levels of TNF
393 in DA.VRA4 rats affect the susceptibility to PD-like pathology and together with IL-1β and IL-
394 5 exacerbates α-Syn pathological spread and neurodegeneration. In fact, inhibition of soluble
395 TNF has been shown to attenuate microglia and astrocyte activation and protect against
396 dopaminergic neurodegeneration in a rat 6-OHDA model of PD[42]. Further investigation would
397 be necessary to assess if TNF inhibition could modulate neuroinflammation,
398 neurodegeneration and α-Syn pathology in the rAAV-α-syn+PFF model.
399

400 As all models, the rAAV-α-Syn+PFF PD rat model has both strengths, as highlighted earlier,
401 and limitations. A limitation of models using intracranial injections is the physical damage and
402 blood-brain barrier disruption possibly causing changes in immune populations, independent
403 of what is injected. In order to control for immune responses not related to α-Syn, injections
404 of an empty vector in SN and vehicle in striatum was used for the control groups. We chose
405 an empty vector since we and others have observed that the commonly used rAAV-GFP
406 control vector elicits a neuroinflammatory response[14,20], and a fluorescent control protein
407 would also interfere with flow cytometry. As control for PFF, we chose to use vehicle, since
408 we have found that bovine serum albumin elicits a neuroinflammatory response[14] and other
409 studies report that α-Syn monomers and saline are comparable controls for the PFF model in
410 rats[28]. We have previously investigated the effects of differential CIITA expression on PD-like
411 α-Syn pathology and neurodegeneration at 8-weeks post SN injection of rAAV6-α-Syn in the
412 rAAV-α-Syn+PFF model[14] and microglia profile and neurodegeneration 12-weeks post SN
413 injection using a rAAV-α-Syn vector only[13]. Studies have shown that there is an inflammatory
414 response ongoing prior to neurodegeneration in animal models[27,28,43] and in PD patients[10].
415 Therefore, we chose to include an earlier time point in our current study; 4 weeks post nigral
416 injection of rAAV-α-Syn. Since α-Syn pathology and MHCII+ microglial cells are widespread in
417 the brain in the rAAV-α-Syn+PFF model[14] we included entire hemispheres for flow cytometric
418 analyses in the current study. Consequently, it is possible that region-specific differences
419 affected by CIITA levels or responses to α-Syn are missed.
420
421 In conclusion, our results show that CIITA levels alter molecules linking the innate and
422 adaptive immune system in both local and peripheral immune populations that could explain
423 the increased susceptibility to α-Syn-induced neurodegeneration and pathological protein
424 spread observed in DA.VRA4 rats with naturally occurring lower CIITA levels[13,14] (Fig. 6). We
425 also observed continuously elevated levels of serum TNF in DA.VRA4 rats. To assess if these
426 elevated TNF levels are causally related to the increased susceptibility to α-Syn-induced PD-
427 like pathology requires further studies. Collectively, our work together with other
428 experimental and human studies highlight the complexity and importance of understanding
429 the link between innate and adaptive immune responses in PD.

430 MATERIALS AND METHODS

431 Experimental design

432 To investigate the effects of differential expression of CIITA we used wt DA rats and a congenic
433 DA.VRA4 rat strain with lower expression levels of CIITA and MHCII[13]. Male rats entered the
434 study at 12±1 weeks of age and a total of 77 rats were included with 6-9 rats/group. We used
435 a combination of viral overexpression of human α-Syn combined with seeding of human PFF,
436 adapted from Thakur et al[44]. Rats were injected with a rAAV6 vector carrying human α-Syn[16]
437 into the SN followed two weeks later by an injection of human α-Syn PFF in the striatum (Fig.
438 1)[14]. Animals were sacrificed at 4- and 8-weeks post nigral injection for collection of brain,
439 serum and CSF samples. Six animals per strain and time point were used for flow cytometric
440 analysis of brain and blood samples and 2-3 animals per strain and time point were used for
441 qualitative IHC validation of α-Syn expression, TH loss, α-Syn pathology and MHCII
442 upregulation. Naïve rats (n=6 per strain) were sacrificed at 12±1 weeks of age and used as
443 baseline for cytokine levels and flow cytometric analyses of blood and brain. Two rats (1 naïve
444 DA and 1 DA.VRA4 α-Syn 8 week) were excluded from flow cytometry analysis of brain due
445 to unsatisfactory perfusion and blood-filled ventricles, respectively. One DA rat from the 8-
446 week α-Syn group was excluded from flow cytometry analysis for both blood and brain due
447 to a clogged capillary during stereotactic surgery. One DA rat from the 8-week control group
448 was excluded for flow cytometry analysis of blood due to inadequate number of events.

449

450 Animals

451 The DA.VRA4 strain was generated by transfer of the VRA4 locus from the PVG strain to a DA
452 background[45]. Rats were housed 2-3 per cage in "type III high" individually ventilated cages
453 with free access to standard rodent chow and water and kept in a pathogen-free and climate-
454 controlled environment with a 12-hour light/dark cycle at the Biomedical Center in Lund. All
455 procedures were approved by the local ethics committee in the Malmö-Lund region and
456 specified in permit 18037-19.

457

458 Viral vectors

459 rAAV6 carrying human α-Syn under transcriptional regulation by the Synapsin-1 promotor
460 and the woodchuck hepatitis virus posttranscriptional regulatory element (WPRE) was

461 generated as previously described[16] and injected at a concentration of 1.3E+10 gc/µl. The
462 same vector but without the human α-Syn gene was used as a control and injected at a
463 concentration of 1.7E+10 gc/µl. Concentration was determined by ITR-qPCR.
464
465 Pre-formed fibrils
466 Human α-Syn PFF were produced as previously described[46] and stored at -80°C until use. PFF
467 were diluted to a concentration of 2.5 µg/µl in sterile DPBS and sonicated for 6 min with 1 s
468 ON/1 s OFF pulses at 70% power using a Q125 sonicator and cup horn (Qsonica, U.S.). The
469 gross structure of PFF before and after sonication were imaged using transmission electron
470 microscopy. PFF were diluted to a concentration of 0.025 µg/µl and transferred to a
471 hexagonal pattern 400 mesh cupper grid with a pioloform film reinforced with a carbon coat,
472 for 20 min at room temperature (RT). Samples were stabilized with uranyl acetate for 1 min.
473 Excess uranyl acetate was removed and the grids were left to dry for at least 5 min prior to
474 imaging using a FEI Tecnai Spirit BioTWIN transmission electron microscope (FEI, U.S.).
475
476 Surgical procedure
477 Rats were anaesthetized with 5% and maintained with 1-3% isoflurane (Isoflo vet, Orion
478 Pharma) with a 2:1 mixture of O_2: NO_2 during the surgical procedure. Rats were attached to
479 a stereotactic frame with a flat-skull position and 0.2 ml. Marcain (2.5 mg/ml, Aspen Nordic,
480 Denmark) was subcutaneously (s.c.) injected under the scalp for local analgesia. Burr holes
481 were created using a dental drill. For nigral injections, 3 µl rAAV6-(-) or rAAV6-α-Syn was
482 injected in the following coordinates taken from bregma[47]; Anterior/posterior (A/P) -5.3 mm,
483 medial/lateral (M/L) ±1.7 mm and dorsal/ventral (D/V) -7.2 mm. For striatal injections, 3 µl
484 PFF (2.5 µg/µl) or DPBS as control was injected using the following coordinates relative to
485 bregma[47]; A/P -0.4 mm, M/L ±3.0 mm and D/V -4.5 mm. Injections were made unilaterally in
486 the right hemisphere using a 10 µl Hamilton syringe (Hamilton, U.S.) fitted with a glass
487 capillary. Injections were made with a flow rate of 0.5 µl/2 min and the capillary was left for
488 2 min after the injection before it was slowly retracted. The wound was sutured using surgical
489 staples. Metacam (1 mg/kg) (Boehringer Ingelheim Animal Health, Germany) was injected s.c.
490 for post-operative analgesia. The rats were left to recover in clean cages and monitored for
491 48 h post-surgery.

492

493 ## Tissue collection

494 Rats were euthanized by intraperitoneal injection of 200-300 mg/kg sodium pentobarbital
495 (APL, Sweden).

496

497 ### Cerebrospinal fluid (CSF) sampling

498 CSF samples were collected at baseline, 4- and 8-weeks post nigral injection from all 77 rats
499 in a stereotactic frame with an approximate 50-60° downward flex of the head. A midline
500 incision was made over the neck and muscles covering the cisterna magna were severed using
501 a scalpel. CSF samples were aspirated using a 27G scalp vein set (Vygon, France) by inserting
502 the bevel of the needle perpendicular to the cisterna magna. CSF was collected into protein
503 LoBind tubes (Eppendorf, Germany), immediately put on dry ice and stored at -80°C until
504 analysis. CSF samples contaminated with blood were excluded from analysis.

505

506 ### Serum and whole blood collection

507 Blood from naïve, 4- and 8-week time points from all 77 rats included in the study was
508 collected by cardiac puncture. For cytokine analysis, serum was prepared by leaving whole
509 blood undisturbed at RT for 30-60 min followed by centrifugation for 10 min at 4°C and
510 2,000xg. Serum was aliquoted into protein LoBind tubes (Eppendorf, Germany) and stored at
511 -80°C until analysis. Whole blood was collected into K3E EDTA coated tubes (BD, U.S.) and
512 stored at 4°C for 3-4 h until preparation for flow cytometric analysis.

513

514 ### Brain processing for immunohistochemistry and flow cytometry

515 After CSF and blood sampling, rats were transcardially perfused with 0.9% saline (w/v) with
516 the descending aorta clamped using hemostatic forceps for at least 5 min or until no blood
517 was visible. For IHC analysis, rats were subsequently perfused with ice-cold 4%
518 paraformaldehyde (PFA) for 5 min and the brains post-fixed in 4% PFA at 4°C overnight (O/N)
519 followed by cryopreservation in PBS containing 30% sucrose (w/v) and 0.01% sodium azide
520 (w/v), pH 7.2 until sectioning. For flow cytometric analysis, brains were collected into ice-cold
521 Roswell Park Memorial Institute 1640 medium without phenol red (Gibco/Thermo Fischer
522 Scientific, U.S.) and stored at 4°C for a maximum of 3 h until processing.

523

524 ## Sample preparation for Flow cytometry

525 ### Brain sample collection and homogenization

526 Hemispheres of freshly collected brains were separated and put into a 7 ml glass dounce
527 tissue grinder (DWK, Germany) with 3-5 ml ice-cold 1x Hank's Balanced Salt Solution (HBSS)
528 without calcium, magnesium or phenol red (Gibco/Thermo Fischer Scientific, U.S.), pH 7.0-
529 7.4. Each hemisphere was homogenized on ice using the large clearance pestle followed by
530 the small clearance pestle until complete homogenization. The glass dounce tissue grinder
531 set was washed with detergent and dried between samples. Homogenized samples were
532 passed through a 100 µm nylon cell strainer (Falcon, U.S.) into a 50 ml conical tube to remove
533 any remaining large debris. 1x HBSS (pH 7.0-7.4) was added until a total volume of 12 ml was
534 reached and samples were kept on ice until separation of myelin and brain mononuclear cells.

535

536 ### Brain mononuclear cell isolation by gradient separation

537 Brain mononuclear cells were isolated and myelin removed using an adapted two-layer
538 density gradient protocol[48,49]. A 100% stock isotonic Percoll (SIP) was prepared by diluting
539 Percoll (GE Healthcare, U.S.) 9:1 in 10x HBSS (Gibco/Thermo Fischer Scientific, U.S.) and 35%
540 SIP was prepared by diluting 100% SIP 0.35:1 in 1x HBSS pH 7.0-7.4. Homogenized brain
541 samples were centrifuged for 5 min at 4°C and 400xg, the supernatant was discarded and the
542 pellet was thoroughly resuspended in 16 ml of 35% SIP. The cell suspension was carefully
543 layered with 5 ml of 1x HBSS pH 7.0-7.4 and centrifuged for 30 min at 4°C and 800xg without
544 brake. The HBSS layer (top), myelin layer (between HBSS and 35% SIP) and 35% SIP was
545 aspirated and the pelleted isolated brain mononuclear cells were washed in 10 ml of 1x HBSS
546 pH 7.0-7.4 and resuspended in ice-cold fluorescence-activated cell sorting (FACS) buffer.

547

548 ### Blood sample preparation

549 Whole blood (200 µl) samples collected in EDTA coated tubes was used for flow cytometric
550 analysis. Red blood cells (RBCs) were lysed by adding 1.8 ml of 1x Pharm Lyse (BD, U.S.) to
551 whole blood cell samples and incubated at RT for 15-20 min. Cells were washed in sterile-
552 filtered PBS (pH 7.2) and resuspended in sterile-filtered ice-cold FACS buffer (2% (w/v) bovine
553 serum albumin fraction V (Roche, Switzerland) and 0.01% sodium azide (w/v) in PBS (pH 7.2)).

554

555 Antibody staining for flow cytometric analysis

556 FcγII receptors on blood and brain samples were blocked by adding anti-rat CD32 diluted
557 1:200 and incubated for 5 min at 4°C. 50 µl of cell suspension was stained using an antibody
558 cocktail (Table 1) diluted in Brilliant Stain Buffer (BD, U.S.). Cells were incubated with
559 antibodies for 30 min at 4°C in dark followed by washing in sterile PBS (pH 7.2). Cells were
560 resuspended in 250 µl of sterile FACS buffer containing DRAQ7 diluted 1:1,000 prior to
561 analysis.

562

563 **Table 1. Antibodies, viability marker and compensation beads used for flow cytometry**

Antigen/ Target	Species specificity	Fluorochrome/ Conjugation	Clone	Isotype/ Host	Dilution	Company
CD45	Rat	APC-eFluor 780	OX1	Mouse IgG1, κ	1:100	Invitrogen (47-0461-82)
CD3	Rat	BV421	1F4	Mouse IgM, κ	1:200	BD Horizon (563948)
CD4	Rat	BV605	OX-35	Mouse IgG2a, κ	1:200	BD OptiBuild (740369)
CD8a	Rat	PE-Cy7	OX8	Mouse IgG1, κ	1:200	Invitrogen (25-0084-82)
CD11b	Rat	PE	WT.5	Mouse IgA, κ	1:200	BD Pharmingen (562105)
MHCII RT1B	Rat	Alexa Fluor 647	OX-6	Mouse IgG1, κ	1:400	Bio-Rad (MCA46A647)
CD86	Rat	BV711	24F	Mouse IgG1, κ	1:100	BD OptiBuild (743215)
FcγRII	Rat	-	D34-485	Mouse IgG1, κ	1:200	BD Pharmingen (550270)
Compensation	Mouse, κ	-	-	-	-	BD CompBeads (552843)
Viability/ dsDNA	-	DRAQ7	-	-	1:1,000	Invitrogen (D15106)

564

565 Samples were analyzed using an LSR Fortessa (BD, U.S.), configuration specified in Table 2.
566 Compensation was performed using BD CompBeads (BD, U.S.) and prepared according to
567 manufacturer's instructions. Fluorescence minus one, unstained and unstained cells with
568 viability dye were included for each recording session and for each sample type (blood or
569 brain) and used to set gates. Gating strategy for brain and blood samples can be seen in
570 Supplementary Fig. 2a and 3a. Microglial cells were gated as $CD45^{dim}$CD11b+ in brain samples.

571 Infiltrating macrophages/monocytes (CD45^{high}CD11b+) and T lymphocytes (CD45+CD3+) in
572 brain samples were rare with <1,000 events/hemisphere. Myeloid population in blood was
573 gated as CD45+CD11b+ and T lymphocytes as CD45+CD3+. Th cells were gated as CD4+ and
574 cytotoxic T lymphocytes as CD8+. Data was analyzed using FlowJo software version 10.8.1
575 (BD, U.S.). All analyses were done on freshly isolated tissue and recorded during multiple
576 sessions. 4-6 rats were used at each recording session (equal number of DA and DA.VRA4 rats
577 per session) from the same experimental group (naïve/control/α-Syn) and time point (4- or
578 8- weeks). To minimize variation introduced by the instrument or sample preparation from
579 each session all comparisons from full groups are made from percentages or normalized
580 values.
581
582 **Table 2. Configuration of the LSR Fortessa used for flow cytometric analysis and filters used for**
583 **recording of isolated blood and brain cells.**

Laser	Filter	Fluorochrome
Blue – 488 nm	780/60	PE-Cy7
	695/40	-
	610/20	-
	575/26	PE
	530/30	-
	488/10	SSC
Red – 640 nm	780/60	APC-eFluor 780
	730/45	DRAQ7
	670/30	Alexa Fluor 647
Violet – 405 nm	780/60	-
	710/50	BV711
	660/20	-
	610/20	BV605
	525/50	-
	442/46	BV421

584
585 Immunohistochemistry
586 Fixed brains were coronally sectioned on a Microm HM450 freezing microtome (Thermo
587 Scientific, U.S.) with 35 µm thickness in series of 12 and stored in Walter's antifreeze solution
588 at 4°C until IHC staining. All stainings were done on free floating sections except for proteinase
589 K treated α-Syn staining which was done on mounted sections on gelatin-coated glass slides.
590 Sections were rinsed with PBS or 0.1% PBS with Triton-X 100 (v/v) (PBST) between all
591 incubation steps. For proteinase K resistant α-Syn aggregates, sections were incubated with

592 5 µg/ml Proteinase K diluted in TBS (Thermo Fischer Scientific, U.S.) for 1 h at RT prior to
593 quenching. For 3,3´-diaminobenzidine (DAB) stainings sections were quenched with 3% H_2O_2
594 (v/v) and 10% MetOH (v/v) in PBS. Sections were blocked with 10% serum (same species as
595 secondary antibody) in 0.3% PBST. Primary antibody was diluted in 0.3% PBST with 5% serum
596 (same species as secondary antibody) and incubated at 4°C O/N. On the following day sections
597 were incubated with biotinylated secondary antibody and incubated for 1 or 2 h at RT (DAB
598 or Fluorescence, respectively). All antibodies used for IHC are found in Table 3. For DAB
599 stainings, horseradish peroxidase conjugated avidin/biotin-complex (Vector laboratories,
600 U.S.) was prepared according to manufacturer's instructions and added to the sections for 30
601 min at RT. A DAB substrate kit (Vector laboratories, U.S.) was prepared according to
602 manufacturer's instructions and used as a chromogen for visualization. DAB sections were
603 mounted on gelatin-coated glass slides, dehydrated and coverslipped using Pertex (Histolab,
604 Sweden). Fluorescently stained sections were coverslipped using PVA/DABCO and stored at
605 4°C in dark. Brightfield overview images of TH and human α-Syn were acquired using an
606 Olympus VS-120 virtual slide scanner (Olympus, Japan). Brightfield images of pS129 α-Syn and
607 proteinase K treated human α-Syn in SN was acquired using an Olympus BX53 (Olympus,
608 Japan). MHCII+ microglia cells were imaged using a Leica SP8 scanning confocal microscope
609 (Leica, Germany).
610
611 **Table 3. List of antibodies used for immunohistochemistry**

Antigen/Secondary antibody	Host	Dilution	Company
Human α-Syn	Mouse	1:1,000	Santa Cruz (sc-12767)
Biotinylated anti-mouse	Horse	1:200	Vector Laboratories (BA-2001)
TH	Rabbit	1:1,000	EMD Millipore (AB152)
pS129 α-Syn	Rabbit	1:2,000	Abcam (ab51253)
Biotinylated anti-rabbit	Goat	1:200	Vector Laboratories (BA-1000)
MHCII	Mouse	1:500	Abcam (ab23990)
Alexa Fluor 488 anti-mouse	Donkey	1:200	Abcam (ab150105)

612

613 Cytokine analysis

614 Cytokine analysis in serum and CSF was performed using the V-PLEX Proinflammatory panel
615 2 Rat Kit from Mesoscale diagnostics (MSD, U.S.) according to manufacturer's instructions.
616 The plates were washed using PBS with 0.05% Tween-20 between incubation steps. Serum
617 samples were diluted 4-fold and CSF samples 2-fold. Plates were read on a MESO QuickPlex
618 SQ 120 analyzer (MSD, U.S.). Results were analyzed using the Discovery Workbench software

619 version 4.0.13 (MSD, U.S.). The number of samples used for cytokine analysis differs as a
620 consequence for available wells on the MSD plate. All samples were run in duplicates and the
621 mean value was used for analysis. If only one replicate was detected it was included in the
622 analysis. If both replicates were undetected for a sample the non-detected (ND) value was
623 replaced with the lowest quantifiable value for the specific cytokine. If duplicates for more
624 than one sample was undetected for a group no statistical comparisons were made due to
625 uncertainty of the results, however, all detected values are presented. If all samples were
626 undetected for a group it is indicated by "ND".
627

628 Statistical analyses

629 Statistical analyses were conducted using the GraphPad Prism software version 9.3.1 (San
630 Diego, CA, U.S.). Quantile-quantile plot of residuals was used to determine the use of
631 parametric or non-parametric tests. Data in figures is presented as mean ± SD and individual
632 values. Comparisons between contralateral and ipsilateral hemispheres was done by paired
633 Student's t-test. Unpaired Student's t-test was used to compare control and α-Syn+PFF
634 groups within strain or naïve/control/α-Syn+PFF between strains. Data in text is presented as
635 (mean1 ± SD1 vs mean2 ± SD2, p-value, 95% CI of difference [lower limit, upper limit]). A
636 significance level of $\alpha<0.05$ was used for all analyses.

637 DATA AVAILABILITY

638 All original data is available from the corresponding author upon reasonable request.

639 ACKNOWLEDGEMENTS

640 This study was supported by MuliPark – A Strategic Research Area at Lund University, and we
641 acknowledge; the AAV Vector Lab platform and Jenny G. Johansson for production of the
642 rAAV constructs, the FACS Platform and Anna Hammarberg for assistance of Flow cytometry
643 experiments, the MESO QuickPlex Platform and Shorena Janelidze for access to the MESO
644 QuickPlex SQ 120 analyzer and the Confocal Microscope Platform for access to the Leica SP8
645 scanning confocal microscope. Lund University Bioimaging Centre (LBIC), Lund University, is
646 gratefully acknowledged for providing experimental resources. We acknowledge the Lund
647 Stem Cell Center Imaging Facility, Lund University, for access to the Olympus VS-120 virtual
648 slide microscope. We also acknowledge the following funding bodies: The Swedish research

council, MultiPark, NEURO Sweden, Hjärnfonden, Bertil och Ebon Norlins Stiftelse, Åke Wibergs stiftelse and Parkinson Research Foundation.

ATHOR CONTRIBUTION

F.B., I.J.F. and M.S. designed the study. K.C.L. produced α-Syn pre-formed fibrils. F.B. and I.J.F. performed stereotactic injections, sample collection and flow cytometric recordings. F.B. performed enzyme-linked immunosorbent assays. Data was analyzed by F.B., K.G., M.S. and L.B. All authors contributed to the manuscript.

COMPETING INTEREST

The authors declare no competing interest.

REFERENCES

1 Poewe, W. *et al.* Parkinson disease. *Nat Rev Dis Primers* **3**, 17013, doi:10.1038/nrdp.2017.13 (2017).

2 Ascherio, A. & Schwarzschild, M. A. The epidemiology of Parkinson's disease: risk factors and prevention. *Lancet Neurol* **15**, 1257-1272, doi:10.1016/S1474-4422(16)30230-7 (2016).

3 Hirsch, E. C. & Hunot, S. Neuroinflammation in Parkinson's disease: a target for neuroprotection? *Lancet Neurol* **8**, 382-397, doi:10.1016/S1474-4422(09)70062-6 (2009).

4 Hamza, T. H. *et al.* Common genetic variation in the HLA region is associated with late-onset sporadic Parkinson's disease. *Nat Genet* **42**, 781-785, doi:10.1038/ng.642 (2010).

5 Kannarkat, G. T. *et al.* Common Genetic Variant Association with Altered HLA Expression, Synergy with Pyrethroid Exposure, and Risk for Parkinson's Disease: An Observational and Case-Control Study. *NPJ Parkinsons Dis* **1**, doi:10.1038/npjparkd.2015.2 (2015).

6 Yu, E. *et al.* Fine mapping of the HLA locus in Parkinson's disease in Europeans. *NPJ Parkinsons Dis* **7**, 84, doi:10.1038/s41531-021-00231-5 (2021).

7 Huppa, J. B. & Davis, M. M. T-cell-antigen recognition and the immunological synapse. *Nat Rev Immunol* **3**, 973-983, doi:10.1038/nri1245 (2003).

8 Brochard, V. *et al.* Infiltration of CD4+ lymphocytes into the brain contributes to neurodegeneration in a mouse model of Parkinson disease. *J Clin Invest* **119**, 182-192, doi:10.1172/JCI36470 (2009).

9 Gate, D. *et al.* CD4(+) T cells contribute to neurodegeneration in Lewy body dementia. *Science* **374**, 868-874, doi:10.1126/science.abf7266 (2021).

10 Sulzer, D. *et al.* T cells from patients with Parkinson's disease recognize alpha-synuclein peptides. *Nature* **546**, 656-661, doi:10.1038/nature22815 (2017).

11 Lindestam Arlehamn, C. S. *et al.* alpha-Synuclein-specific T cell reactivity is associated with preclinical and early Parkinson's disease. *Nat Commun* **11**, 1875, doi:10.1038/s41467-020-15626-w (2020).

688 12 Williams, G. P. *et al.* Targeting of the class II transactivator attenuates inflammation
689 and neurodegeneration in an alpha-synuclein model of Parkinson's disease. *J*
690 *Neuroinflammation* **15**, 244, doi:10.1186/s12974-018-1286-2 (2018).
691 13 Jimenez-Ferrer, I., Jewett, M., Tontanahal, A., Romero-Ramos, M. & Swanberg, M.
692 Allelic difference in Mhc2ta confers altered microglial activation and susceptibility to
693 alpha-synuclein-induced dopaminergic neurodegeneration. *Neurobiol Dis* **106**, 279-
694 290, doi:10.1016/j.nbd.2017.07.016 (2017).
695 14 Jimenez-Ferrer, I. *et al.* The MHC class II transactivator modulates seeded alpha-
696 synuclein pathology and dopaminergic neurodegeneration in an in vivo rat model of
697 Parkinson's disease. *Brain Behav Immun* **91**, 369-382, doi:10.1016/j.bbi.2020.10.017
698 (2021).
699 15 Swanberg, M. *et al.* MHC2TA is associated with differential MHC molecule expression
700 and susceptibility to rheumatoid arthritis, multiple sclerosis and myocardial
701 infarction. *Nat Genet* **37**, 486-494, doi:10.1038/ng1544 (2005).
702 16 Decressac, M., Mattsson, B., Lundblad, M., Weikop, P. & Bjorklund, A. Progressive
703 neurodegenerative and behavioural changes induced by AAV-mediated
704 overexpression of alpha-synuclein in midbrain dopamine neurons. *Neurobiol Dis* **45**,
705 939-953, doi:10.1016/j.nbd.2011.12.013 (2012).
706 17 Sommer, A. *et al.* Infiltrating T lymphocytes reduce myeloid phagocytosis activity in
707 synucleinopathy model. *J Neuroinflammation* **13**, 174, doi:10.1186/s12974-016-
708 0632-5 (2016).
709 18 George, S. *et al.* T Cells Limit Accumulation of Aggregate Pathology Following
710 Intrastriatal Injection of alpha-Synuclein Fibrils. *J Parkinsons Dis* **11**, 585-603,
711 doi:10.3233/JPD-202351 (2021).
712 19 Williams, G. P. *et al.* CD4 T cells mediate brain inflammation and neurodegeneration
713 in a mouse model of Parkinson disease. *Brain*, doi:10.1093/brain/awab103 (2021).
714 20 Harms, A. S. *et al.* Peripheral monocyte entry is required for alpha-Synuclein induced
715 inflammation and Neurodegeneration in a model of Parkinson disease. *Exp Neurol*
716 **300**, 179-187, doi:10.1016/j.expneurol.2017.11.010 (2018).
717 21 Gonzalez De La Cruz, E. *et al.* MhcII Regulates Transmission of alpha-Synuclein-
718 Seeded Pathology in Mice. *Int J Mol Sci* **23**, doi:10.3390/ijms23158175 (2022).
719 22 McGeer, P. L., Itagaki, S., Boyes, B. E. & McGeer, E. G. Reactive microglia are positive
720 for HLA-DR in the substantia nigra of Parkinson's and Alzheimer's disease brains.
721 *Neurology* **38**, 1285-1291, doi:10.1212/wnl.38.8.1285 (1988).
722 23 Tansey, M. G. *et al.* Inflammation and immune dysfunction in Parkinson disease. *Nat*
723 *Rev Immunol* **22**, 657-673, doi:10.1038/s41577-022-00684-6 (2022).
724 24 Subbarayan, M. S., Hudson, C., Moss, L. D., Nash, K. R. & Bickford, P. C. T cell
725 infiltration and upregulation of MHCII in microglia leads to accelerated neuronal loss
726 in an alpha-synuclein rat model of Parkinson's disease. *J Neuroinflammation* **17**, 242,
727 doi:10.1186/s12974-020-01911-4 (2020).
728 25 Harms, A. S. *et al.* MHCII is required for alpha-synuclein-induced activation of
729 microglia, CD4 T cell proliferation, and dopaminergic neurodegeneration. *J Neurosci*
730 **33**, 9592-9600, doi:10.1523/JNEUROSCI.5610-12.2013 (2013).
731 26 Basurco, L. *et al.* Microglia and astrocyte activation is region-dependent in the alpha-
732 synuclein mouse model of Parkinson's disease. *Glia*, doi:10.1002/glia.24295 (2022).

733 27 Earls, R. H. *et al.* Intrastriatal injection of preformed alpha-synuclein fibrils alters
734 central and peripheral immune cell profiles in non-transgenic mice. *J*
735 *Neuroinflammation* **16**, 250, doi:10.1186/s12974-019-1636-8 (2019).
736 28 Harms, A. S. *et al.* alpha-Synuclein fibrils recruit peripheral immune cells in the rat
737 brain prior to neurodegeneration. *Acta Neuropathol Commun* **5**, 85,
738 doi:10.1186/s40478-017-0494-9 (2017).
739 29 Karikari, A. A. *et al.* Neurodegeneration by alpha-synuclein-specific T cells in AAV-
740 A53T-alpha-synuclein Parkinson's disease mice. *Brain Behav Immun* **101**, 194-210,
741 doi:10.1016/j.bbi.2022.01.007 (2022).
742 30 Thome, A. D. *et al.* Ex vivo expansion of dysfunctional regulatory T lymphocytes
743 restores suppressive function in Parkinson's disease. *NPJ Parkinsons Dis* **7**, 41,
744 doi:10.1038/s41531-021-00188-5 (2021).
745 31 Bhatia, D. *et al.* T-cell dysregulation is associated with disease severity in Parkinson's
746 Disease. *J Neuroinflammation* **18**, 250, doi:10.1186/s12974-021-02296-8 (2021).
747 32 Bas, J. *et al.* Lymphocyte populations in Parkinson's disease and in rat models of
748 parkinsonism. *J Neuroimmunol* **113**, 146-152, doi:10.1016/s0165-5728(00)00422-7
749 (2001).
750 33 Kustrimovic, N. *et al.* Parkinson's disease patients have a complex phenotypic and
751 functional Th1 bias: cross-sectional studies of CD4+ Th1/Th2/T17 and Treg in drug-
752 naive and drug-treated patients. *J Neuroinflammation* **15**, 205, doi:10.1186/s12974-
753 018-1248-8 (2018).
754 34 Chen, Y. *et al.* Clinical correlation of peripheral CD4+cell subsets, their imbalance and
755 Parkinson's disease. *Mol Med Rep* **12**, 6105-6111, doi:10.3892/mmr.2015.4136
756 (2015).
757 35 Sommer, A. *et al.* Th17 Lymphocytes Induce Neuronal Cell Death in a Human iPSC-
758 Based Model of Parkinson's Disease. *Cell Stem Cell* **23**, 123-131 e126,
759 doi:10.1016/j.stem.2018.06.015 (2018).
760 36 Mamula, D., Khosousi, S., He, Y., Lazarevic, V. & Svenningsson, P. Impaired migratory
761 phenotype of CD4(+) T cells in Parkinson's disease. *NPJ Parkinsons Dis* **8**, 171,
762 doi:10.1038/s41531-022-00438-0 (2022).
763 37 Chen, X., Hu, Y., Cao, Z., Liu, Q. & Cheng, Y. Cerebrospinal Fluid Inflammatory
764 Cytokine Aberrations in Alzheimer's Disease, Parkinson's Disease and Amyotrophic
765 Lateral Sclerosis: A Systematic Review and Meta-Analysis. *Front Immunol* **9**, 2122,
766 doi:10.3389/fimmu.2018.02122 (2018).
767 38 Kwilasz, A. J., Grace, P. M., Serbedzija, P., Maier, S. F. & Watkins, L. R. The
768 therapeutic potential of interleukin-10 in neuroimmune diseases.
769 *Neuropharmacology* **96**, 55-69, doi:10.1016/j.neuropharm.2014.10.020 (2015).
770 39 Qin, X. Y., Zhang, S. P., Cao, C., Loh, Y. P. & Cheng, Y. Aberrations in Peripheral
771 Inflammatory Cytokine Levels in Parkinson Disease: A Systematic Review and Meta-
772 analysis. *JAMA Neurol* **73**, 1316-1324, doi:10.1001/jamaneurol.2016.2742 (2016).
773 40 Gordon, R. *et al.* Inflammasome inhibition prevents alpha-synuclein pathology and
774 dopaminergic neurodegeneration in mice. *Sci Transl Med* **10**,
775 doi:10.1126/scitranslmed.aah4066 (2018).
776 41 Fan, Z. *et al.* Systemic activation of NLRP3 inflammasome and plasma alpha-
777 synuclein levels are correlated with motor severity and progression in Parkinson's
778 disease. *J Neuroinflammation* **17**, 11, doi:10.1186/s12974-019-1670-6 (2020).

42 Barnum, C. J. *et al.* Peripheral administration of the selective inhibitor of soluble tumor necrosis factor (TNF) XPro(R)1595 attenuates nigral cell loss and glial activation in 6-OHDA hemiparkinsonian rats. *J Parkinsons Dis* **4**, 349-360, doi:10.3233/JPD-140410 (2014).

43 Duffy, M. F. *et al.* Lewy body-like alpha-synuclein inclusions trigger reactive microgliosis prior to nigral degeneration. *J Neuroinflammation* **15**, 129, doi:10.1186/s12974-018-1171-z (2018).

44 Thakur, P. *et al.* Modeling Parkinson's disease pathology by combination of fibril seeds and alpha-synuclein overexpression in the rat brain. *Proc Natl Acad Sci U S A* **114**, E8284-E8293, doi:10.1073/pnas.1710442114 (2017).

45 Harnesk, K. *et al.* Vra4 congenic rats with allelic differences in the class II transactivator gene display altered susceptibility to experimental autoimmune encephalomyelitis. *J Immunol* **180**, 3289-3296, doi:10.4049/jimmunol.180.5.3289 (2008).

46 Luk, K. C. *et al.* Exogenous alpha-synuclein fibrils seed the formation of Lewy body-like intracellular inclusions in cultured cells. *Proc Natl Acad Sci U S A* **106**, 20051-20056, doi:10.1073/pnas.0908005106 (2009).

47 Paxinos, G. & Watson, C. *Paxinos and Watson's The Rat Brain in Stereotaxic Coordinates*. 7th edn, (Elsevier Academic Press, 2014).

48 Grabert, K. *et al.* Microglial brain region-dependent diversity and selective regional sensitivities to aging. *Nat Neurosci* **19**, 504-516, doi:10.1038/nn.4222 (2016).

49 Grabert, K. & McColl, B. W. Isolation and Phenotyping of Adult Mouse Microglial Cells. *Methods Mol Biol* **1784**, 77-86, doi:10.1007/978-1-4939-7837-3_7 (2018).

804 FIGURES AND FIGURE LEGENDS

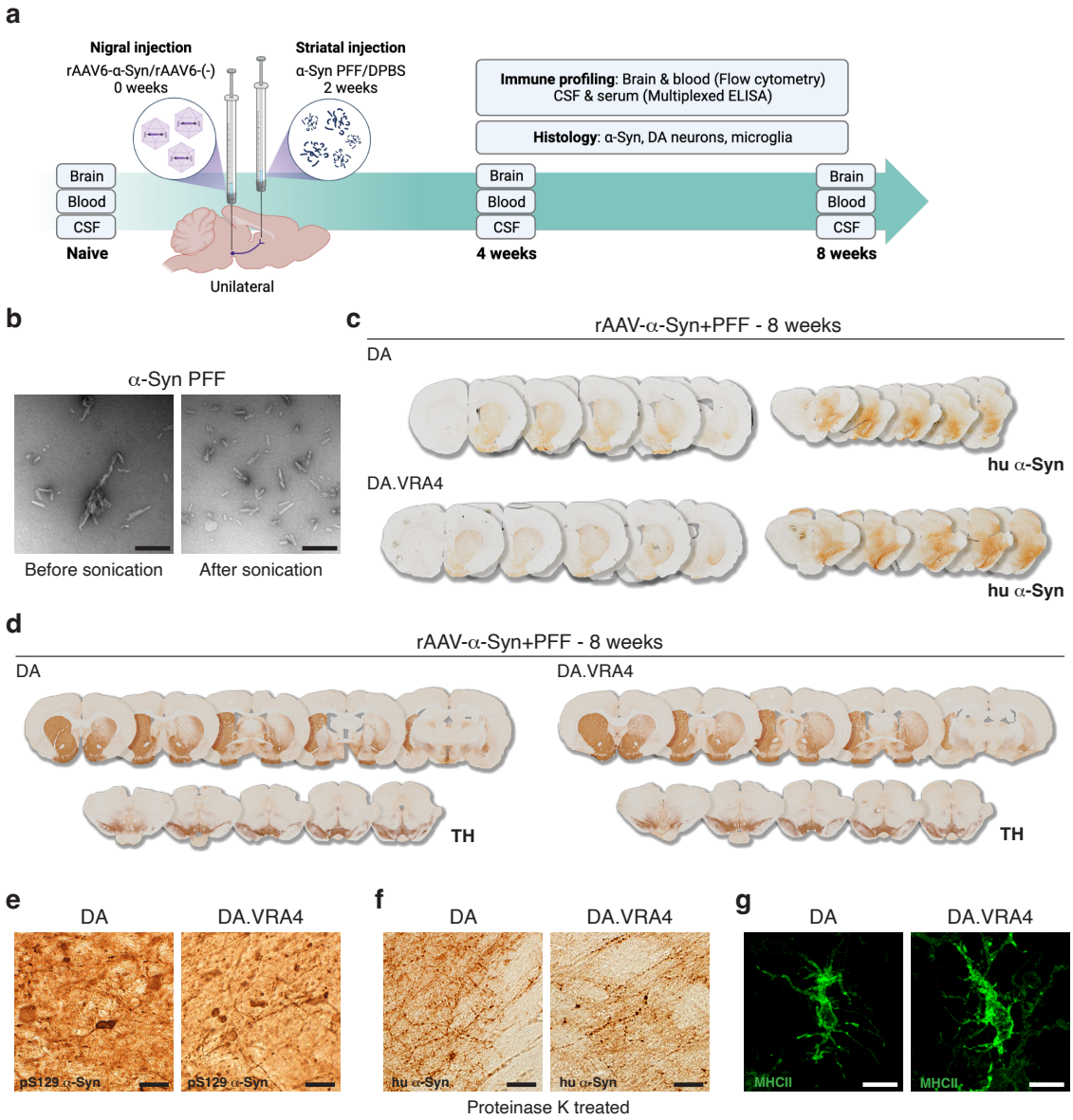

805

806 **Fig. 1. α-Syn overexpression combined with striatal seeding of α-Syn pre-formed fibrils**
807 **(PFF) leads to TH loss, α-Syn pathology and MHCII upregulation. a** Experimental outline
808 (created with BioRender.com). **b** TEM images of α-Syn PFF before (left) and after (right)
809 sonication; sonicated PFF were used for striatal seeding. Scale bar = 200 nm. **c** Unilateral nigral
810 overexpression of human α-Syn combined with striatal seeding of human PFF results in robust
811 human α-Syn signal in substantia nigra (SN) and striatum. rAAV-α-Syn+PFF injection leads to
812 **d** loss of TH-signal in both striatum and SN, **e** positive signal for phosphorylated α-Syn on
813 serine residue 129 (pS129 α-Syn) and **f** proteinase K resistant α-Syn aggregates. **e-f**
814 Representative images from 8 weeks ipsilateral SN, scale bar = 20 µm. **g** rAAV-α-Syn+PFF

injection leads to upregulation of MHCII on microglia, representative image from 8 weeks ipsilateral midbrain, scale bar = 10 µm.

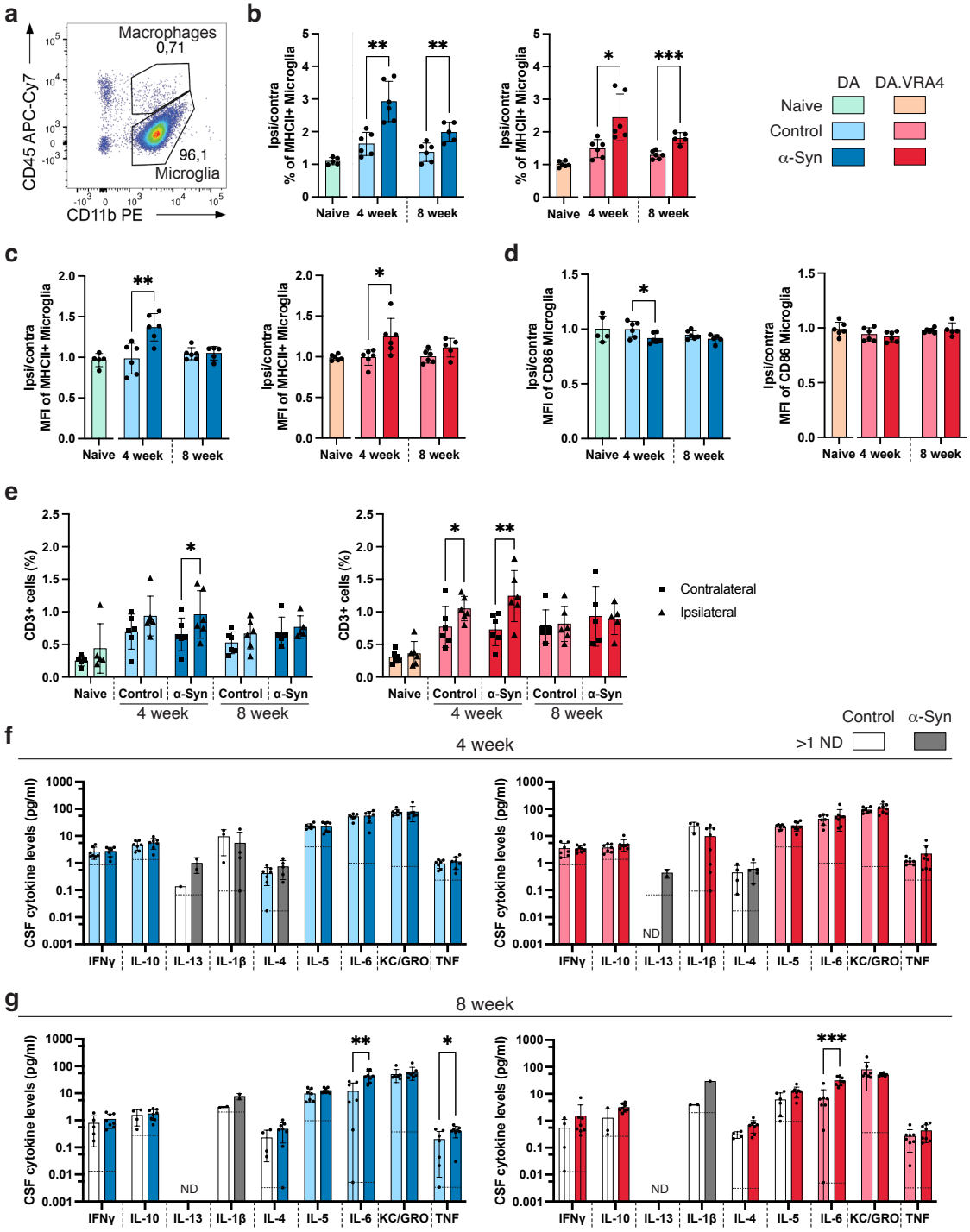

Fig. 2. Local effects of rAAV-α-Syn+PFF on microglial MHCII expression, infiltrating lymphocytes and CSF cytokine profiles. a Gating of microglia (CD45^{dim}CD11b+) and infiltrating macrophages/monocytes (CD45^{high}CD11b+) in brain samples. **b** Normalized (ipsilateral/contralateral hemisphere) percentage of MHCII+ microglia is higher in rAAV-α-

822 Syn+PFF injected animals compared to control in both DA (left) and congenic DA.VRA4 (right)
823 rats. **c** MHCII levels determined by normalized median fluorescence intensity (MFI) values in
824 DA (left) and DA.VRA4 (right) rats are higher after 4- but not 8-weeks post nigral α-Syn
825 overexpression. **d** Normalized MFI values of CD86 in DA (left) and DA.VRA4 (right) rats. **e**
826 Stereotactic injection leads to increased percentage of T lymphocytes (CD45+CD3+) in DA
827 (left) and congenic DA.VRA4 (right) rats. **b-e** Naïve (DA n=5, DA.VRA4 n=6), 4-week; control
828 (DA n=6, DA.VRA4 n=6) and α-Syn (DA n=6, DA.VRA4 n=6), 8-week; control (DA n=6, DA.VRA4
829 n=6) and α-Syn (DA n=5, DA.VRA4 n=5). **f-g** Cytokine levels in cerebrospinal fluid (CSF) 4- and
830 8-weeks post nigral injection, respectively, in DA (left) and DA.VRA4 (right) rats. α-Syn
831 injection results in elevated IL-6 levels in both DA and DA.VRA4 and TNF in DA.VRA4 at 8
832 weeks. No statistical analysis was done if >1 value/group was non-detected (ND). The limit
833 for lowest quantifiable value for each cytokine is indicated by a horizontal dashed line. Groups
834 with all values non-detected are indicated by "ND". 4-week; control (DA n=7, DA.VRA4 n=7)
835 and α-Syn (DA n=7, DA.VRA4 n=8), 8-week; control (DA n=7), DA.VRA4 n=8) and α-Syn (DA
836 n=8, DA.VRA4 n=8). **b-d, f-g** Unpaired Student's t-test. **e** Paired Student's t-test. *$p < 0.05$, **p
837 < 0.01 and ***$p < 0.001$. Data presented as mean ± SD with individual values.

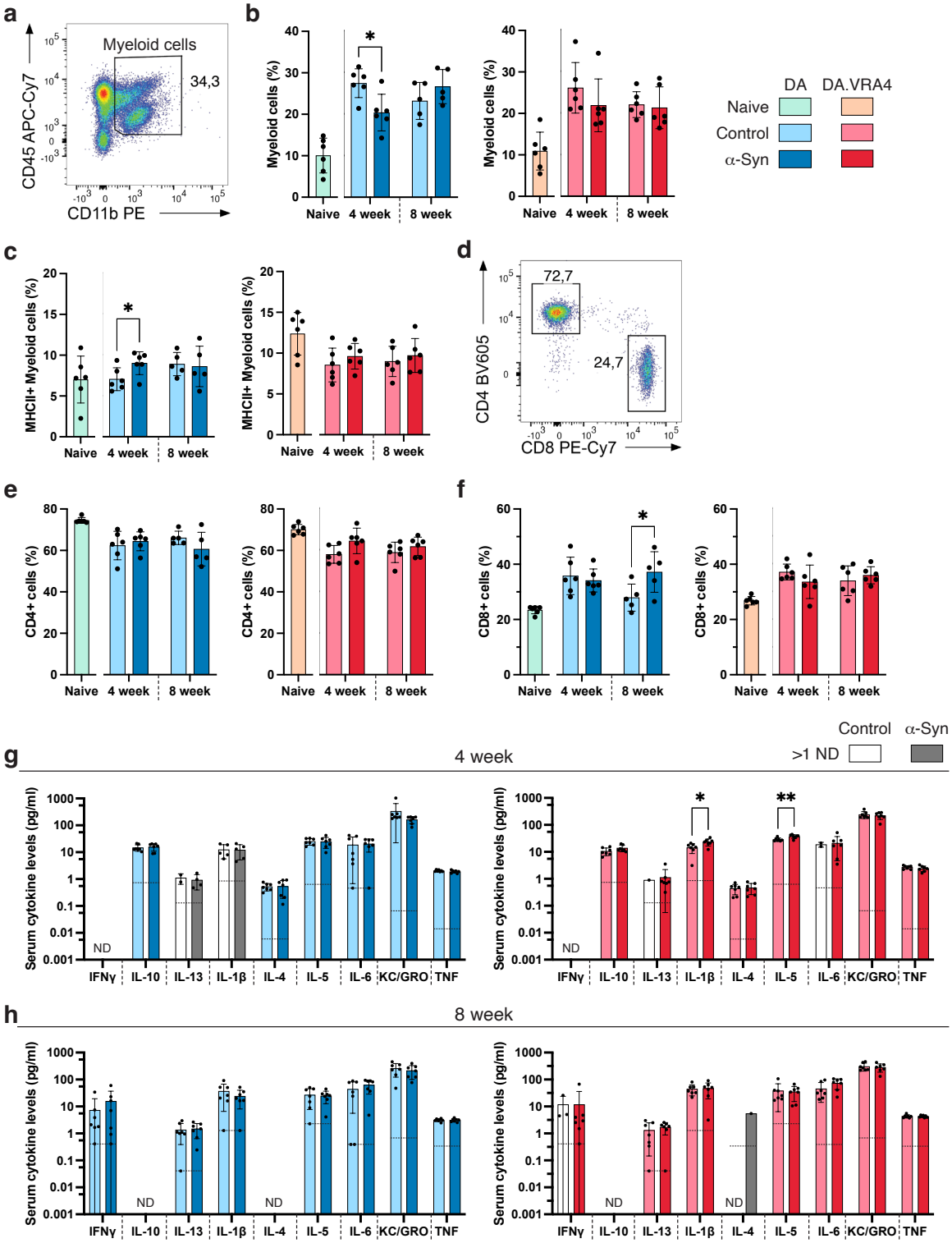

Fig. 3. Systemic effects of rAAV-α-Syn+PFF on blood myeloid cells' MHCII expression, circulating lymphocytes and serum cytokine profiles. **a** Gating of myeloid cells (CD45+CD11b+) in blood. **b** Overall percentage of myeloid cells in DA (left) and DA.VRA4 (right) at 4- and 8-weeks. **c** Percentage of MHCII+ myeloid cells is reduced in DA rats (left) α-Syn group compared to control but unaltered in congenic DA.VRA4 rats (right). **d** Gating of

844 CD4+ or CD8+ T lymphocytes (CD45+CD3+ cells). **e** Overall percentage of CD4+ T lymphocytes
845 in blood does not change after rAAV-α-Syn+PFF injection in the brain of DA (left) or DA.VRA4
846 (right) rats. **f** Percentage of CD8+ T lymphocytes increase in α-Syn group at 8 weeks in DA
847 (left) rats. **g-h** rAAV-α-Syn+PFF injection results in increased serum IL-1β and IL-5 levels in
848 DA.VRA4 rats (right) after 4 weeks, n=7/group. **h** No change in serum cytokine levels is
849 observed at 8 weeks post nigral rAAV-α-Syn injection in DA (left) or DA.VRA4 (right) rats,
850 n=7/group. No statistical analysis was done if >1 value/group was ND. Groups with all values
851 non-detected are indicated by "ND". The limit for lowest quantifiable value for each cytokine
852 is indicated by a horizontal dashed line. **a-f** Naïve (DA n=6, DA.VRA4 n=6), 4 week; control (DA
853 n=6, DA.VRA4 n=6) and α-Syn (DA n=6, DA.VRA4 n=6), 8 week; control (DA n=5, DA.VRA4 n=6)
854 and α-Syn (DA n=5, DA.VRA4 n=6). **b,c and e-h** Unpaired Student's t-test. *$p < 0.05$, **$p <$
855 0.01. Data presented as mean ± SD with individual values.
856

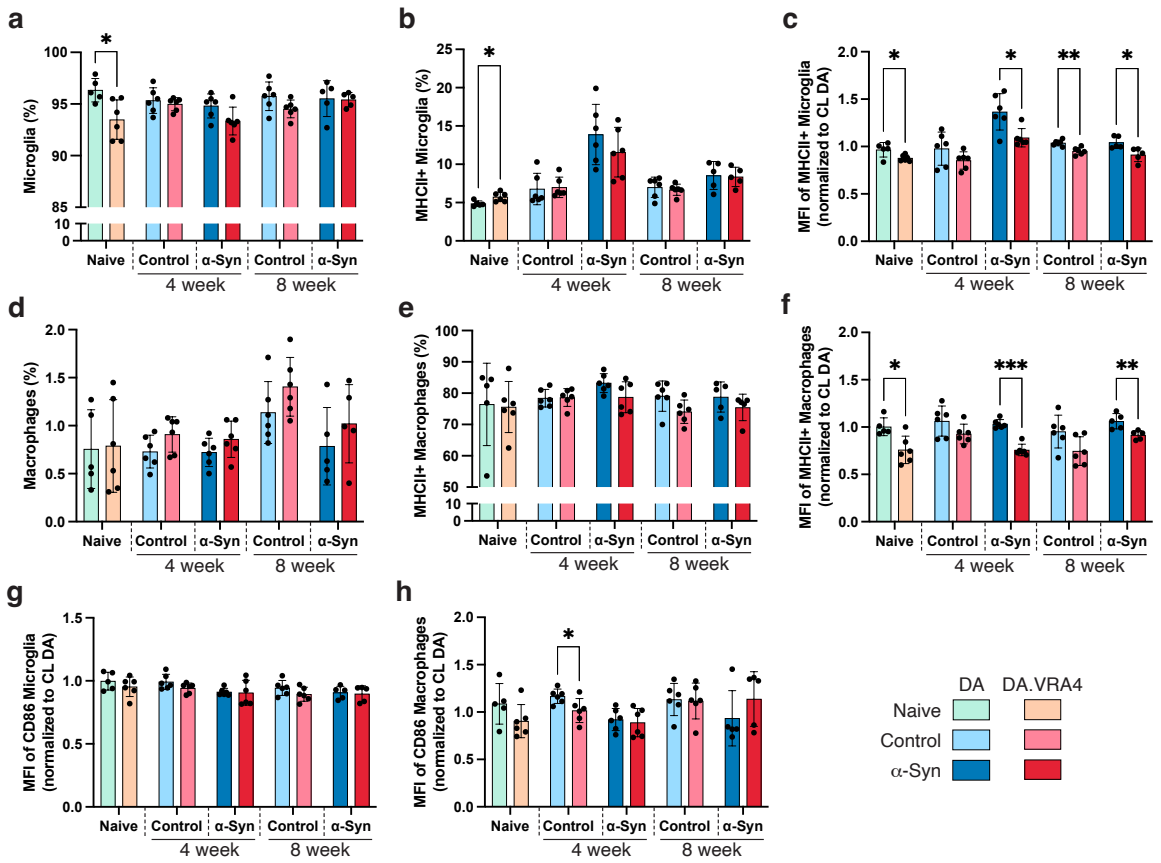

Fig. 4 CIITA regulates local MHCII levels on both microglia and infiltrating macrophages in response to rAAV-α-Syn+PFF. a Total percentage of microglia ($CD45^{dim}CD11b+$) is reduced in naïve DA rats compared to DA.VRA4 rats with lower CIITA levels. **b** Percentage of MHCII+ microglia is higher in naïve DA compared to DA.VRA4. **c** Congenic DA.VRA4 rats with lower CIITA have reduced MHCII MFI levels on microglia independent of α-Syn, normalized to contralateral (CL) DA values. **d** Percentage of infiltrating macrophages/monocytes ($CD45^{high}CD11b+$) and **e** MHCII+ macrophages are not regulated by differing CIITA levels. **f** DA.VRA4 rats have reduced MHCII MFI levels on infiltrating macrophages compared to DA independent of rAAV-α-Syn+PFF injections (normalized to CL DA). **g** Normalized microglial CD86 MFI levels is not regulated by CIITA. **h** CD86 MFI levels (normalized to CL DA) are not regulated by CIITA in response to α-Syn. Naïve (DA n=5, DA.VRA4 n=6), 4-week; control (DA n=6, DA.VRA4 n=6) and α-Syn (DA n=6, DA.VRA4 n=6), 8-week; control (DA n=6, DA.VRA4 n=6) and α-Syn (DA n=5, DA.VRA4 n=5). Data presented as mean ± SD with individual values. Unpaired Student's t-test. *$p < 0.05$, **$p < 0.01$ and ***$p < 0.001$.

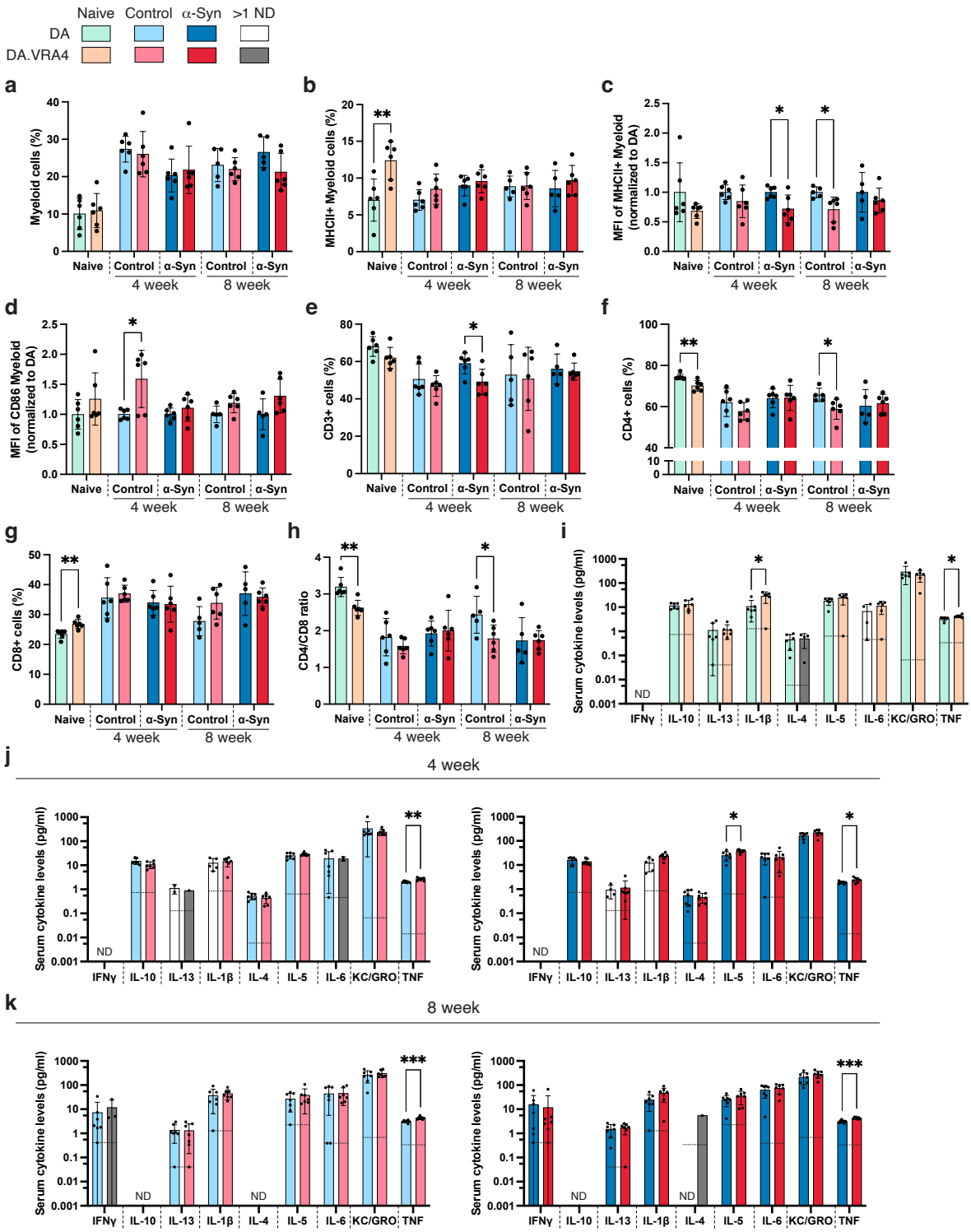

Fig. 5. CIITA regulates MHCII levels on blood myeloid cells and TNF levels in serum. a The proportion of myeloid cells (CD45+CD11b+) in blood is not regulated by CIITA. **b** Naïve DA.VRA4 rats with less CIITA have an increased proportion of MHCII+ myeloid cells compared to DA. **c** CIITA regulates MHCII MFI levels in circulating myeloid cells. **d** CD86 MFI levels are not regulated by CIITA in response to α-Syn. **e** Reduced percentage of T lymphocytes

879 (CD45+CD3+) in rats with lower CIITA levels 4 weeks after rAAV-α-Syn SN injection. **f-h** Naïve
880 congenic DA.VRA4 rats with lower CIITA levels have less CD4+ but more CD8+ T lymphocytes
881 (CD45+CD3+) leading to a reduced CD4/CD8 ratio. **a-h** Naïve (DA n=6, DA.VRA4 n=6), 4 week;
882 control (DA n=6, DA.VRA4 n=6) and α-Syn (DA n=6, DA.VRA4 n=6), 8 week; control (DA n=5,
883 DA.VRA4 n=6) and α-Syn (DA n=5, DA.VRA4 n=6). **i-k** Congenic DA.VRA4 rats with less CIITA
884 have increased TNF levels in serum independent of α-Syn. No statistical analysis was done if
885 >1 value/group was ND. The limit for lowest quantifiable value for each cytokine is indicated
886 by a horizontal dashed line. Groups with all values non-detected are indicated by "ND". **i**
887 n=6/group. **j-k** n=7/group. Data presented as mean ± SD with individual values. Unpaired
888 Student's t-test. *$p < 0.05$, **$p < 0.01$ and ***$p < 0.001$.
889

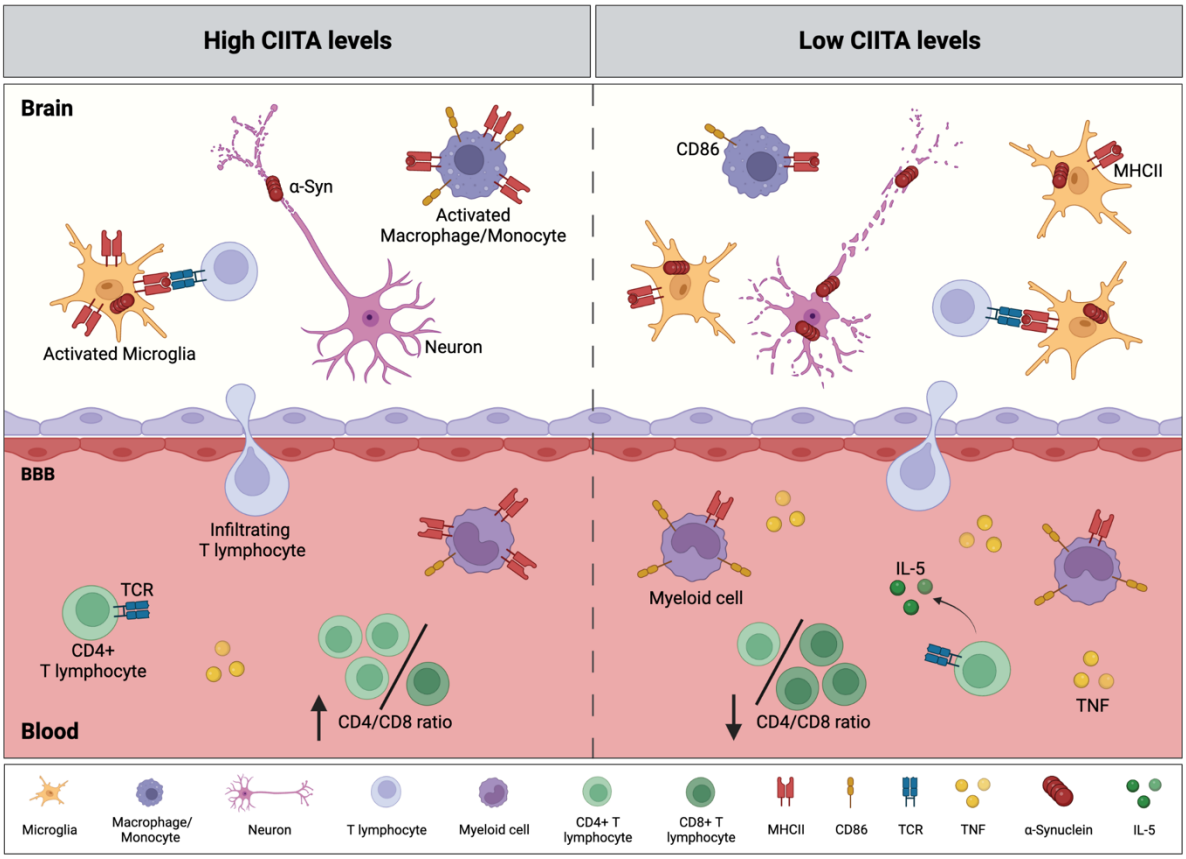

Fig. 6. CIITA regulates baseline immune populations that could affect the susceptibility to PD-like pathology and exacerbate α-Syn propagation. Lower CIITA levels are associated with motor impairments[13,14], neurodegeneration[13,14] and exacerbated α-Syn pathological spread[14] in response to α-Syn. Reduced CIITA levels are also associated with lower MHCII levels on microglia[13,14] and myeloid cells (both in brain and blood, reported in the current study). In addition to an increased number of activated microglia (determined by morphology[13] and MHCII positive cells in striatum[13,14]) in response to α-Syn, the current study also reveals that reduced CIITA levels are associated with increased numbers of MHCII+ microglia in brain and MHCII+ myeloid cells in circulation in naïve rats, which could influence the susceptibility to PD-like pathology. We believe that the increased number of activated microglia in rats with low CIITA levels are important to consider in terms of susceptibility and progression of PD-like pathology. Infiltrating T lymphocytes could be presented with processed α-Syn peptides in the brain, leading to an adaptive immune response (lower CIITA levels are associated with elevated levels of IL-5 in serum in response to α-Syn). α-Syn reactive T lymphocytes in circulation have been reported in PD by *ex vivo* studies in PD patients[9,10]. CIITA levels regulated CD4/CD8 ratio in blood in naïve rats and TNF levels in serum. If TNF levels have an

907 impact on susceptibility and progression of α-Syn seeded PD-like pathology requires further
908 investigation. The illustration was created with BioRender.com.